Cu_2O nanoparticles: Radiation synthesis, and photocatalytic activity

LIN Xiangfeng[1] ZHOU Ruimin[1,*] SHENG Xiaohai[2] ZHANG Jianqiang[1]

[1] *Shanghai Applied Radiation Institute, Shanghai University, Shanghai 201800, China*

[2] *National Engineering Research Center for Nanotechnology, Shanghai 200241, China*

Abstract Cu_2O nanocrystals were synthesized by irradiating an aqueous solution of $CuSO_4 \cdot 5H_2O$ (1.25g), polyvinyl alcohol (PVA, 0.8 g), and isopropanol (3.1 mL). The products were characterized by powder XRD, TEM and SEM. Methyl orange degradation under visible light using the Cu_2O nanocrystals as catalyst was studied by UV-Vis absorption method. The results show that the products are nanocrystals of pure Cu_2O. Morphology and size of the nanoparticles are affected by the irradiation dose and pH value of the initial solution. Octahedral Cu_2O nanocrystals of 116 nm in size can be obtained at the initial pH of 8.0 and 280-kGy irradiation. The nanocrystals have excellent catalytic activity for photodegradation of the methyl orange solution bubbled at the air-flow rate of 750 $mL \cdot min^{-1}$, due to the large {111} facets of octahedral Cu_2O particles.

Key words E-beam irradiation, Cuprous oxide, Nanoparticles, Photodegradation

1 Introduction

Since 1998 when Hara M *et al.* [1] reported that Cu_2O, which can be activated by visible lights due to its p-type band gap of 2.17 eV, could be used as photocatalyst for water splitting, it has been applied in solar energy conversion[2], organic synthesis[3], gas sensors[4–5], and CO oxidation[6].

Cu_2O nanocrystal in different shapes have been synthesized by a number of methods, such as chemical deposition[7], electro-deposition[8], and irradiation with microwaves[9] and γ-rays[10–12]. In the chemical deposition and microwave irradiation, Cu^{2+} ions were reduced into Cu_2O by reducer, while electrodeposition, and ionizing radiations (γ-rays, E-beams) are direct reducer in themselves. Reducing Cu^{2+} to Cu_2O can be completed by E-beam irradiation in several or tens of minutes, or by hours of γ-irradiation[11, 12]. In this work, Cu_2O nanoparticles were prepared by E-beam irradiation at room temperature. The products were characterized by powder X-ray diffraction (XRD), Fourier transform infrared (FT-IR) spectroscopy, transmission electron microscopy (TEM), scanning electron microscopy (SEM), and UV-Vis absorption spectroscopy. Photocatalytic activity of the Cu_2O nanoparticles was evaluated by decomposing methyl orange under visible light, and factors affecting the photodegradation efficiency were investigated.

2 Experimental

All chemical reagents, from relevant manufacturers in China, were of analytical grade and used without purification. A 100-mL aqueous solution containing $CuSO_4 \cdot 5H_2O$ (1.25g), polyvinyl alcohol (PVA, 0.8 g), and isopropanol (3.1 mL) was stirred ultrasonically for 20 min, and was adjusted to advisable pH by ammonia (25–28 wt%). The solution was filled into a 22 cm×12 cm plastic bag, and the thickness of the volume was less than 5 mm for irradiation by E-beams from a 2-MeV E-beam accelerator, The solution changed into yellowish orange precipitates, which were collected by centrifugation at 4000 rpm, and washed with Milli-Q water and ethanol, respectively, for three times, and dried in a vacuum oven at 60 °C for 4 h.

Supported by Shanghai Leading Academic Discipline Project (S30109), and the Innovation Foundation of Shanghai University for Ph.D. candidates (SHUCX091033).

* Corresponding author. *E-mail address:* zhourm47@staff.shu.edu.cn

Received date: 2009-09-25

The nanocrystals were characterized by XRD (Rigaku D\Max-2550 powder X-ray diffractometer, Cu Kα, λ =1.54178 Å), FT-IR (Nicolet AVATAR 370), TEM (JEOL-200CX), SEM (Phillips FEI Quanta 200 FEG) and UV-Vis absorption spectroscopy(Httachiu －3010).

Methyl orange was selected as model pollutant. A 500-W halogen-tungsten lamp was used as irradiation light source. The Cu_2O (0.025g) powder, after 30 min in dark to achieve absorption equilibrium, was suspended in 50 $mg \cdot L^{-1}$ methyl orange (100 mL), being bubbled with air during the photodegradation reaction. The solution of 4 mL was sampled at certain intervals and centrifuged at 4000 rpm. The concentration of methyl orange was determined by a TU-1901 spectrophotometer (Beijing Purkinje General Instrument Co. Ltd., China).

3 Results and Discussion

Radiolysis of water generates active intermediates of e^-_{aq}, $H^{\cdot}$, $^{\cdot}OH$[13], etc. (Eq.(1)). As a powerful reducing radical the hydrated electrons reduce Cu^{2+} into Cu^+ (Eq.(2)), which quickly form a unstable CuOH with OH^-, and further decompose into Cu_2O (Eq.(3)). This suggests that the CuOH is an important intermediate during the reaction[14].

$$H_2O \rightarrow e_{aq}^-, H_3O^+, H^{\cdot}, H_2, {}^{\cdot}OH, H_2O_2, \text{etc} \quad (1)$$

$$Cu^{2+} + e_{aq}^- \rightarrow Cu^+ \quad (2)$$

$$2Cu^{2+} + 2OH^- \rightarrow 2CuOH + H_2O \rightarrow Cu_2O + H_2O \quad (3)$$

Fig.1(a) shows powder XRD patterns of Cu_2O octahedrons prepared at pH 8.0 and irradiated to 280 kGy by 7 mA E-beams. The diffraction peaks at 2θ = 29.77°, 36.59°, 42.52°, 52.84°, 61.72°, 73.88°, and 77.85°correspond to the (110), (111), (200), (211), (220), (311) and (222) crystal plane, respectively, with the peak at 2θ = 36.59° being the strongest in intensity. This is consistent with the standard material (JCPDS No.74-1230), indicating that the cubic phase Cu_2O is of a cuprite structure. No peak of impurities, such as Cu or CuO, was found in the XRD patterns, indicating that the obtained particles are pure Cu_2O. In the FT-IR spectrum of the same sample (Fig.1b), the absorption peak at 623 cm^{-1} is assigned to the Cu-O vibration. The position is slightly shifted, due to small particles (~16 nm) coexisting with the octahedrons[15,16].

From TEM and SEM images (Fig. 2) of the same Cu_2O sample (pH 8.0, 280 kGy), the particles are sized at about 16 nm and 116 nm. Fig.2(b) shows the Cu_2O octahedral particles. Some particles clearly display hollow portions, duo probably to ammonia, and this will be further described in later text.

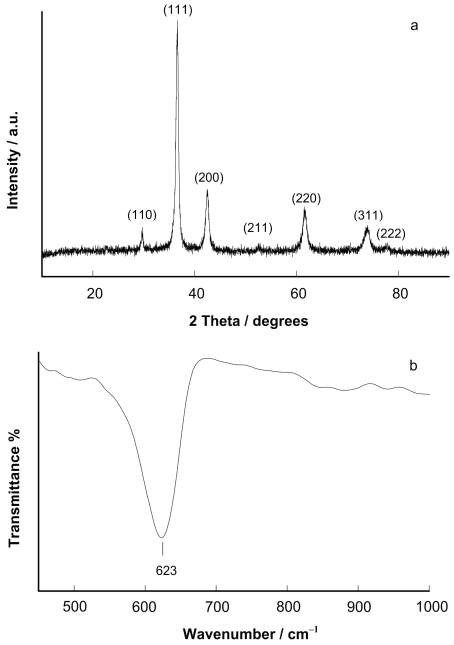

Fig.1 Powder XRD patterns (a) and FI-IR spectrum (b) of Cu_2O octahedrons prepared at pH 8.0 and 280-kGy irradiation.

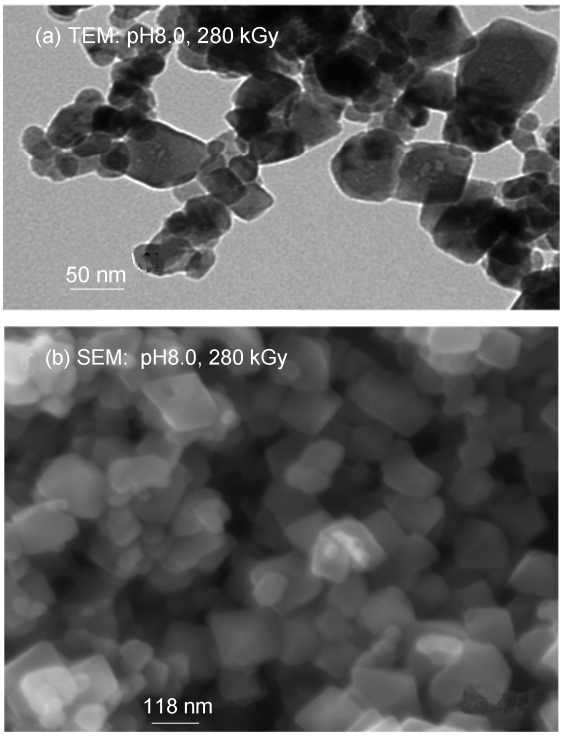

Fig. 2 TEM (a) and SEM (b) images of Cu_2O octahedrons synthesized at pH 8.0 and by 280-kGy irradiation.

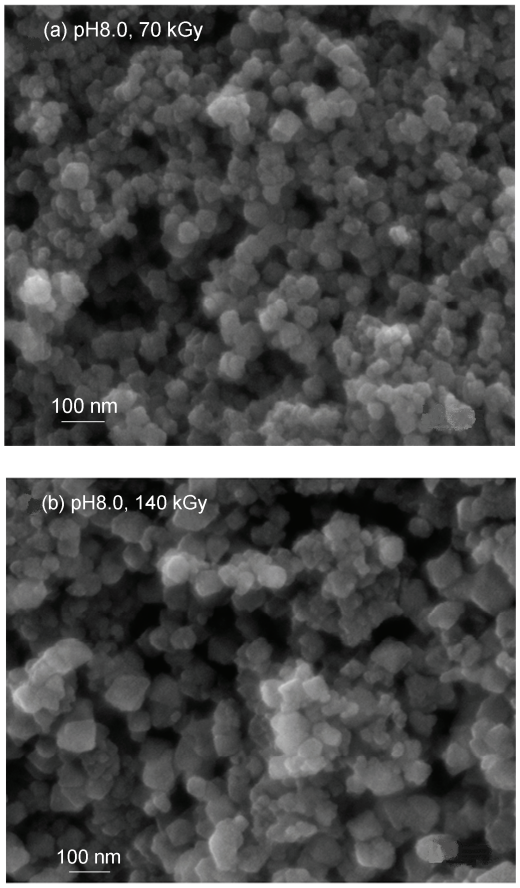

Fig.3 SEM images of the products by (a) 70-kGy irradiation and (b)140-kGy irradiation.

Fig. 3 shows SEM images of the Cu_2O particles obtained by irradiating the same solution as above to 70 and 140 kGy with the 7 mA E-beams. The nanocrystals produced by 70-kGy irradiation are in irregular shapes (Fig. 3a), with their sizes varying from about 10 to 48 nm. The 140-kGy (Fig. 3b) particles are sized at about 11–78 nm, with some particles exhibiting an octahedral morphology, among the disordered nanoparticles. As shown in Fig.(2b), the 280-kGy irradiation produced dominantly the 116-nm octahedral nanoparticles, with smaller nanoparticles (16 nm) adsorbed on surfaces of the octahedrons.

Based on the SEM analysis, it can be speculated that Cu_2O octahedrons are formed by aggregating small crystals. Because the e_{aq}^- reducing Cu^{2+} produces a large number of the disordered Cu_2O nuclei, which served as the seeds to form the octahedral Cu_2O with {111} surfaces through Ostwald ripening[17,18]. During the crystal growth, because the crystal morphology is controlled by the slowest growth rate of (111) plane to form the Cu_2O octahedron, the crystal faces with high growth rate vanishes in the final morphology. The PVA utilized as a capping agent in aqueous solution-based crystal growth[19] can also prevent the crystal growth from happening, and control the nanoparticle sizes due to the disturbed growing surface. The PVA gel helps the homogeneous distribution of the cations in the polymeric network structures[19,20] and adsorbs nonspecifically onto solid surfaces[21]. And the PVA gel stabilizes the Cu_2O particles, and prevents further crystal growth in water.

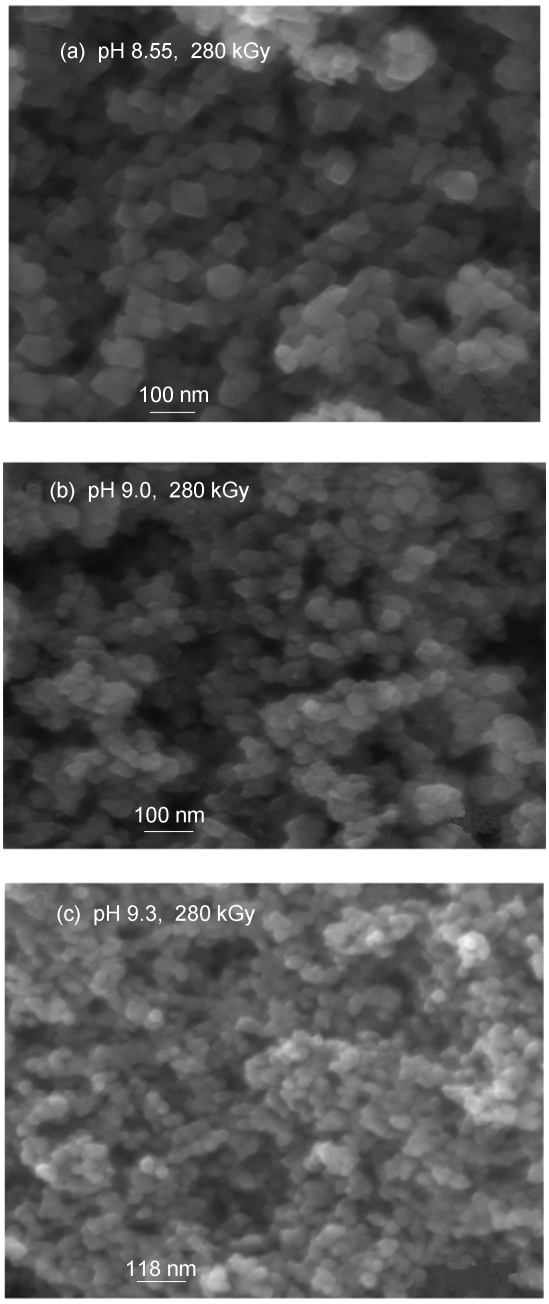

Fig.4 SEM images of the Cu_2O particles prepared at different pH values of the initial solution and irradiated to 280 kGy.

pH value is a main factor in wet chemical processing. In our work, the initial pH shifting should dramatically change the size and shape of Cu_2O particles. While most of the particles at pH 8.0 are octahedral of about 16 nm or 116 nm as shown in Fig.2(b), size of the particles becomes smaller and their shape changes from octahedron to irregularity with increasing the pH value. As shown in Fig. 4, the particles prepared at initial pH of 8.55 and irradiated to 280 kGy are of octahedral morphology, but are sized at 20 and 85 nm. The particles prepared at initial pH of 9.0 and 9.3 are also smaller than that of pH 8.0, and are of irregular morphology.

The dissolution of Cu_2O in ammonia can lead to a colorless $[Cu(NH_3)_2]^+$, and this is important for morphology observation of the Cu_2O nanoparticles when they undergo color changes during the E-beam irradiation. The ammonia was initially used to adjust pH value of the solution, and the radiation-synthesized Cu_2O nanoparticles were then dissolved by enriched ammonia, which is similar to the wet chemical etching. With increased concentration of ammonia, hence increased pH value, the etching speed should increase dramatically. Under irradiation, the colorless solution at a high initial pH of 9.0 and 9.3 changed to blue in a shorter time. The precipitates in the solution at a high initial pH of 10 disappeared in a 10-min irradiation. The blue color is formed by oxidation of the colorless complex $[Cu(NH_3)_2]^+$ to complex $[Cu(NH_3)_4]^{2+}$. Xu *et al*[22] reported that porous Cu_2O spheres were prepared by dissolving Cu_2O in ammonia. And hollow Cu_xS cages[23] and hollow C_{60} nanobox[24] were fabricated by dissolving of the Cu_2O cores of Cu_2O/Cu_xS or Cu_2O-C_{60} core/shell structures in ammonia.

The growth and etching mechanisms of Cu_2O can be illustrated by the schematic models as shown in Scheme 1.

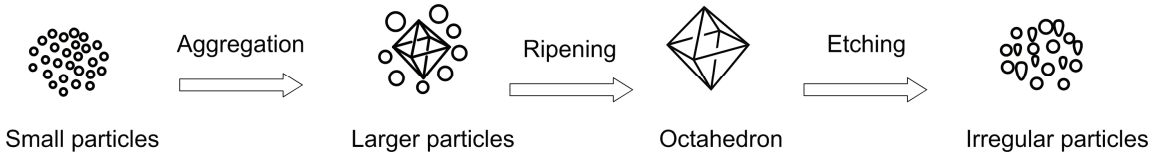

Scheme 1 Schematic of the Cu_2O nanocrystal formation and etching process.

UV-Vis absorption behavior of the Cu_2O nanoparticles prepared at pH 8.0 and synthesized by 280-kGy irradiation is given in Fig. 5. An absorption peak is at 464 nm, which is an obvious blue shift from 570 nm of bulk Cu_2O [15].

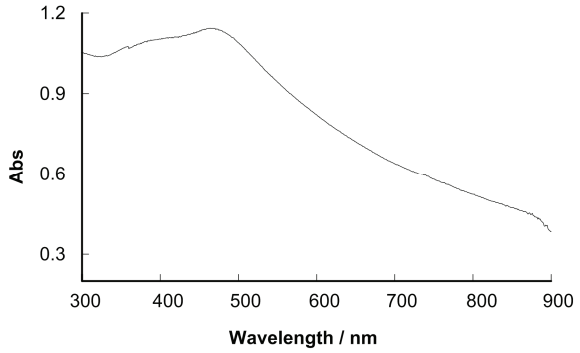

Fig.5 UV-Vis absorption spectra of Cu_2O nanocrystals dispersed in ethanol.

Influence of the preparation conditions on photocatalytic activities of the Cu_2O nanoparticles was investigated by measuring the methyl orange concentration C in the photodegradation, as shown in Fig. 6, where C_0 is the original methyl orange concentrations.

In Fig. 6(a), the Cu_2O octahedral nanoparticles prepared at pH 8.0 with 280-kGy irradiation exhibit a higher photocatalytic activity than the Cu_2O nanoparticles synthesized with the same dose by prepared at pH 8.55, 9.0 and 9.3. The samples were bubbled at an air-flow rate of 750 $mL \cdot min^{-1}$. The results suggest that octahedral Cu_2O nanocrystals with large {111} facets may effectively adsorb the dye molecules at photocatalysis reactions, as previous studies [25,26].

To investigate the air-flow rate effect on photodegradation activity of the nanoparticles, Cu_2O octahedral samples, pH 8.0-prepared and 280-kGy-irradiated, were suspended in the solution of the same initial methyl orange concentration as the sample in

Fig.6(a), and was bubbled at different airflow rates. Fig. 6(b) shows the photodegradation results for the air-flow rate of 0, 345 and 750 mL·min^{-1}. The photodegradation increases with the air-flow rate. The Cu_2O photocatalyst may effectively enhance the adsorption of methyl orange and the dissolved oxygen under air bubbling, which is crucial for photooxidation of the dye during photocatalytic process[27, 28]. It has been reported that the dissolved O_2, $O_2^{\cdot-}$ and $HO_2^{\cdot}$ can react with radicals generated by degradation[29]. The Cu_2O can adsorb a large amount of O_2, including O^- or O^{2-} on the surface[30, 31]. Furthermore, the H_2O_2 can be formed on the surface of Cu_2O by O_2 under visible light irradiation[32–34] . For these reasons, the bubbling air can catalyze photodegradation reaction.

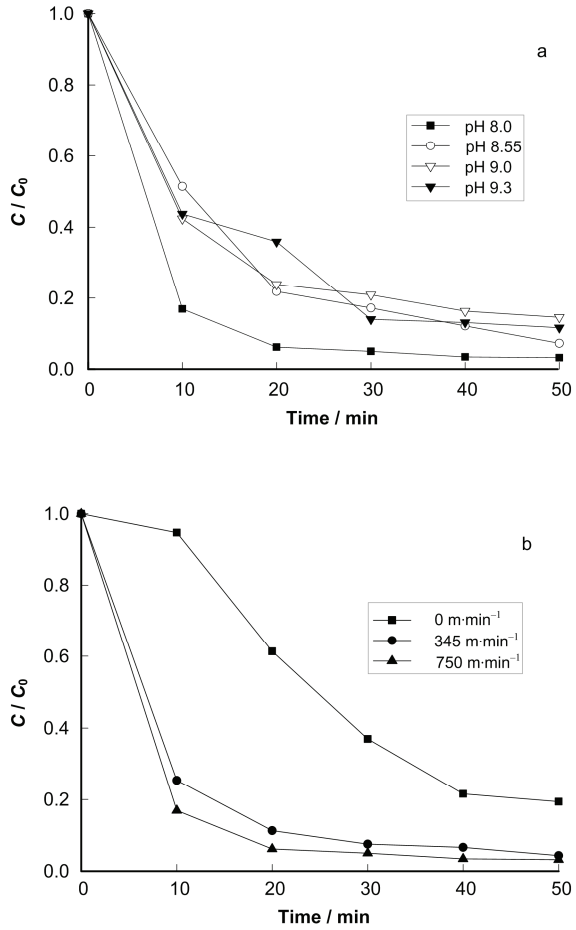

Fig. 6 Methyl orange degradation under visible light using Cu_2O nanoparticles as catalyst. (a) Cu_2O samples prepared from initial solutions of different pH values and 280-kGy E-beam irradiation. The air-flow rate was 750 mL·min^{-1}; (b) at different air-flow rates, with the Cu_2O photocatalysts prepared at pH 8.0 and 280 kGy.

4 Conclusions

Cu_2O nanoparticles have been successfully prepared by E-beam irradiation. Their morphologies are affected by the irradiation dose and pH value of the initial solution. The Cu_2O nanoparticles show activity for photodegradation of methyl orange under visible light. The synthetic conditions and bubbling air-flow rate are correlated with the photocatalytic activity, and the octahedral Cu_2O nanoparticles exhibit high efficiency of the photodegradation at 750 mL·min^{-1} of the air-flow rate.

References

1 Hara M, Kondo T, Komoda M, *et al.* Chem Commun, 1998, **3**: 357−358.

2 Musa A O, Akomolafe T, Carter M J. Sol Energy Mater Sol Cells, 1998, **51**: 305−316.

3 Tang B X, Wang F, Li J H, *et al.* J Org Chem, 2007, **72**: 6294−6297.

4 Zhang J, Liu J, Peng Q, *et al.* Chem. Mater, 2006, **18**: 867−871.

5 Zhang H, Zhu Q, Zhang Y, *et al.* Adv Funct Mater, 2007, **17**: 2766−2771.

6 White B, Yin M, Hall A, *et al.* Nano Lett, 2006, **6**: 2095−2098.

7 Wang W Z, Wang G H, Wang X S. Adv Mater, 2002, **14**: 67−69.

8 Sun F, Guo Y P, Song WB, *et al.* J Cryst Growth, 2007, **304**: 425−429.

9 Wu Z C, Shao M W, Zhang W, *et al.* J Cryst Growth, 2004, **260**: 490–493.

10 Chen Q D, Shen X H, Gao H C. J Colloid Interf Sci, 2007, **312**: 272–278.

11 He P, Shen X H, Gao H C. J Colloid Interf Sci, 2005, **284**: 510–515.

12 Miao W F, Liu H R, Zhang Z G, *et al.* Solid State Sci, 2008, **10**: 1322–1326.

13 Belloni J, Mostafavi M, Remita H, *et al.* New J Chem, 1998: 1239–1255.

14 Gou LF, Murphy CJ. J Mater Chem, 2004, **14**: 735–738.

15 Xu Y Y, Chen D R, Jiao X L, *et al.* J Phys Chem C, 2007, 111: 16284–16289.

16 Borgohain K, Murase N, Mahamuni S. J Appl Phys, 2002, **92**: 1292–1297.

17 Roosen A R, Carter W C. Phys A, 1998, **261**: 232–247.

18 Mullin J W. Crystallization, 3rd ed. London (UK): Butterworth-Heinemann press, 1997, 288.

19 Vargeese A A, Joshi S S, Krishnamurthy V N. Cryst Growth Des, 2008, **8**: 1060 –1066.

20 Oaki Y, Imai H. Cryst Growth Des, 2003, **3:** 711–716.

21 Kim W, Robertson R E, Zand R. Cryst Growth Des, 2005, **5**: 513–522.

22 Xu H L, Wang W Z, Wei Zhu. Micropor Mesopor Mat, 2006, **95**: 321–328.

23 Jiao S, Xu L, Jiang K, *et al.* Adv Mater, 2006, **18**: 1174 –1177.

24 Liu D F, Yang S H, Lee S T. J Phys Chem C, 2008, **112**: 7110–7118.

25 Kuo C H, Huang M H. J Phys Chem C, 2008, **112**: 18355–18360.

26 Xu H L, Wang W Z, Wei Zhu. J Phys Chem B, 2006, **110**: 13829−13834.

27 Wong J C S, Linsebigler A, Lu G, *et al.* J Phys Chem, 1995, **99**: 335−344.

28 Schwitzgebel J, Ekerdt J J, Gerischer H, *et al.* J Phys Chem, 1995, **99**: 5633−5638.

29 Ilisz I, Dombi A. Appl Catal A: Gen, 1999, **180**: 35–45.

30 Wood B J, Wise H, Yolles R S. J Catal, 1969, **15**: 355−362.

31 Zhang L S, Li J L, Chen Z G, *et al.* Appl Catal A: Gen, 2006, **299**: 292–297.

32 De Jongh P E, Vanmaekelbergh D, Kelly J J. J Electrochem Soc, 2000, **147**: 486−489.

33 De Jongh P E, Vanmaekelbergh D, Kelly J J. Chem Commun, 1999: 1069−1070.

34 Li J L, Liu L, Yu Y, *et al.* Electrochem Commun, 2004, **6**: 940–943.